PLOS WATER

RESEARCH ARTICLE

Reactivity of Fe-amended biochar for phosphorus removal and recycling from wastewater

Daniel G. Strawn[1]*, **Alex R. Crump**[1], **Derek Peak**[2], **Manuel Garcia-Perez**[3], **Gregory Möller**[1]

1 Department of Soil and Water Systems, University of Idaho, Moscow, Idaho, **2** University of Saskatchewan, Saskatoon, Canada, **3** Department of Biological Engineering, Washington State University, Pullman, Washington, United States of America

* dgstrawn@uidaho.edu

Citation: Strawn DG, Crump AR, Peak D, Garcia-Perez M, Möller G (2023) Reactivity of Fe-amended biochar for phosphorus removal and recycling from wastewater. PLOS Water 2(4): e0000092. https://doi.org/10.1371/journal.pwat.0000092

Editor: Xueming Chen, Fuzhou University, CHINA

Received: December 12, 2022

Accepted: April 3, 2023

Published: April 28, 2023

Data Availability Statement: All data are reported within the summitted manuscript.

Funding: This publication was developed under Assistance Agreement No. 84008701, awarded by the U.S. Environmental Protection Agency (to DS and GM); and under Agreement No. 2020-69012-31871, funded by the U.S. Department of Agriculture (USDA), National Institute of Food and Agriculture (to DS and GM). This work is also supported by the Idaho Agricultural Experiment Station, USDA, NIFA Project Number IDA01711 (to DS and GM). The funders had no role in study design, data collection and analysis, decision to

Abstract

Using biochar to remove phosphorus (P) from wastewater has the potential to improve surface water quality and recycle recovered P as a fertilizer. In this research, effects of iron modification on P sorption behavior and molecular characterization on two different biochars and an activated carbon were studied. A biochar produced from cow manure anaerobic digest fibers (AD) pyrolyzed under NH_3 gas had the greatest phosphate sorption capacity (2300 mg/kg), followed by the activated carbon (AC) (1500 mg/kg), and then the biochar produced from coniferous forest biomass (BN) (300 mg/kg). Modifying the biochars and AC with 2% iron by mass increased sorption capacities of the BN biochar to 2000 mg/kg and the AC to 2300 mg/kg, but decreased sorption capacity of the AD biochar to 1700 mg/kg. Molecular analysis of the biochars using P K-edge X-ray absorption near edge structure (XANES) spectroscopy indicated that calcium phosphate minerals were the predominant species in the unmodified biochar. However, in the Fe-modified biochars, XANES data suggest that P was sorbed as P-Fe-biochar ternary complexes. Phosphorus sorbed on unmodified BN biochar was more available for release (greater than 35% of total P released) than the AD biochar (less than 1%). Iron modification of the BN biochar decreased P release to 3% of its total P content, but in the AD biochar, P release increased from 1% of total P in the unmodified biochar to 3% after Fe modification. Results provide fundamental information needed to advance the use of biochar in wastewater treatment processes and recover it for recycling as a slow-release soil fertilizer.

1. Introduction

Phosphorus (P) is a limited resource that is mined and thus it is imperative that P recycling technologies are developed to support sustainable resource utilization [1]. The current end-of-life cycle for much of the mined P is human or agricultural waste streams such as wastewater treatment plants or confined animal feeding operations. Because of wastewater treatment

publish, or preparation of the manuscript. The research has not been formally reviewed by the funding agencies. The contents of this document do not necessarily reflect the views and policies of the USEPA, nor does USEPA endorse trade names or recommend the use of commercial products mentioned in this document.

Competing interests: I have read the journal's policy and the authors of this manuscript have the following competing interests: D.G. Strawn and G. Moller are named on patents issued to the University of Idaho entitled "Biochar Water Treatment, U.S. Patent No. 10,351,455; 2019." M. Garcia-Perez is named on patents issued to Washington State University entitled "AMORPHOUS CARBONS FOR PHOSPHATE REMOVAL AND METHODS THEREOF; US Patent application 2022081323."

process deficiencies, some of the P ends up in surface waters where, together with nitrogen (N) loading, it promotes algal blooms that impair water quality [2]. To improve the sustainability of P, it is imperative to recover P from wastewater in a form that can be added back to soils as fertilizer [3–7]. Currently, there are major initiatives to explore opportunities to recycle phosphorus from wastewaters (*European Sustainable Phosphorus Platform* http://phosphorusplatform.eu/, and a United States effort called *Sustainable Phosphorus Initiative* https://sustainablep.asu.edu/). Phosphorus recycling from wastewater would close the P supply and reuse cycle, improving sustainability and preventing water quality degradation.

A common treatment method for P removal from wastewater is adding iron or aluminum salts that form metal oxides with high phosphate adsorption capacity [8,9]. For example, reactive filtration injects iron salt solutions to produce highly reactive hydrous ferric oxide coatings on the sand in a moving bed sand filter reactor [9–11]. While effective, the recovered Fe-treatment residual is of limited use for direct application to soils as a fertilizer, thus limiting P recycling [12]. Other technologies, such as struvite precipitation [13], although effective at recovering P and N, do not typically treat water to the low levels required for discharge and have limitations in continuous-flow treatment processes that present challenges for wastewater engineering [14].

An alternative to using salts to promote flocculation and mineral precipitation of P from wastewater is using modified biochar as a solid substrate water treatment reagent. Numerous studies have investigated the potential and challenges of using biochar for wastewater treatment; recent reviews on this topic are Li *et al.* [15], Nobaharan *et al.* [16], Wang *et al.* [17], Xiang *et al.* [18], and the edited book by Mohan *et al.* [19]. To optimize biochar for use in wastewater treatment, biochar is often modified by amending the feedstock pre-pyrolysis. Fewer studies have investigated post pyrolysis biochar modification that may have operational advantages in wastewater treatment practices [13,20–22]. This could be of great practical value when developing adsorbents from commercially available chars. Additionally, only a few of the biochar P recovery papers have documented the availability of the recovered P for release [23], or conducted molecular characterization to learn the species of P on the biochar controlling sorption and release reactions.

Using biochar in water filtration to recover P has the advantage of producing a nutrient-enriched biochar that facilitates P recycling by replacing fertilizers [4,15,20,24–27]. Recent meta-analysis studies have demonstrated that, on average, the application of biochar to soils can lead to a 16% increase in plant productivity(n = 1254) [28], and 4.6 times increase in P availability (n = 108) [29]. A meta-analysis done by Melo *et al.* [30] found that biochar amendment increased plant productivity by an average of 10% compared to traditional fertilizer, suggesting enhanced benefits of biochar to soil properties that promote plant growth. Thus, there is an overall positive benefit to adding biochar to soils, and after biochar use in wastewater treatment, the recovered biochar will be enriched in nutrients, which can offset the need for traditional fertilizers allowing for cost savings that will support the biochar production and soil amendment costs. Another major advantage for soil biochar amendment is that biochar persist in soils for several hundred years [31,32], facilitating a long-term carbon storage process that can decrease the carbon footprint of the water treatment process, even making it carbon-negative [33].

The ability of biochars to remove phosphate from solution by either adsorption or precipitation reactions is dictated by the physical and chemical properties of the biochar, including the specific surface area of the biochar, the amount and types of surface functional groups, and the cation composition [34,35]. Between pH 4 and 9, phosphate is a negatively charged oxyanion with either one or two negatively charged weak acid oxygen moieties. It can attach to positively charged surfaces via electrostatic attraction and covalent bonds, or through formation

of cation bridges that link phosphate to negatively charged surfaces. In most cases, phosphate adsorbs to mineral surfaces through formation of either bidentate or monodentate coordinated inner-sphere bonds [36–38].

The surface charge of biochar is dominated by functional groups that are negatively charged weak acids [35,39,40]. Thus, the adsorption of phosphate anions on these sites most likely occurs through cation bridging, which is enhanced by the adsorption of multivalent cations like Ca^{2+}, Mg^{2+}, Al^{3+} and Fe^{3+} [41,42]. A second reaction process for removal of P from solution is formation of metal-phosphate precipitates, such as Ca-P minerals (e.g., hydroxyapatite) [43,44], Fe-P minerals (e.g., strengite) [45,46], or struvite ($MgNH_4PO_4$) [44,47,48]. Availability of the metal from the modified biochar for phosphate precipitation reactions depends on its availability and species in the modified biochar.

To enhance P removal from solution onto biochar, several biochar modifications have been proposed, including Fe [21,49–57], and alkaline earth metals Mg or Ca [58–64]. Other less common biochar modifications, such as Zr [65,66], polymer modification [40], or creation of a magnetic Fe-doped biochar [67–70] have also been proposed. Metal modifications facilitate formation of biochar-metal bridges between the phosphate anion and the negatively charged weak-acid functional groups on the biochar surfaces, and can also act as nucleation sites for phosphate mineral precipitation [71–73]. For example, a pretreatment of biomass feedstock with Mg^{2+} salts creates Mg-oxide mineral phases in the biochar that facilitate struvite precipitation on the biochar [53,59,64]; and pretreatment with Fe creates nanoparticulate iron oxide minerals (e.g., hydrous ferric oxide) that have a high adsorption affinity for phosphate [52,74]. Zhang *et al.* [74] prepared activated carbon (carbonized coconut shells) with four different iron oxide coatings (magnetite, hematite, goethite, and ferrihydrite). They observed that the goethite-coated activated carbon had the greatest adsorption capacity, which was several times the adsorption capacity reported for raw activated carbon in other studies. Zhang *et al.* [74] also conducted molecular analysis of the adsorbed P on the Fe-treated activated carbon and observed that the phosphate was sorbed as both inner-sphere complexes and as Fe-P surface precipitates, which was similar to the molecular analysis results observed on Fe-modified biochar produced from corn stover feedstock by Liu *et al.* [50]. While biochar modification has been demonstrated to be successful, it adds cost to the treatment. Additionally, the modification can impact the recycling potential of the recovered P because it alters its release behavior and also the modified biochar can have distinct impacts on the soil physicochemical properties.

Wastewater treatment and P recovery on biochar provides an enhanced sustainability opportunity. The recovered P-enriched biochar has four value-added benefits as a soil amendment: 1) improvements to soil physical properties (e.g., water holding capacity); 2) addition of plant nutrients (P, N and others); 3) slow release of nutrients; and 4) addition of soil carbon that can help the global carbon balance challenges [75]. However, the efficacy of recovered phosphorus on biochar for availability to crops is not yet known [76]. If the biochar is modified to maximize removal of phosphate from wastewater using Fe-modification, the sorbed P may not be released to the soil solution to supply nutrients for plant growth. Or, alternatively, it could be a beneficial slow-release P source for plant nutrient needs [23,77,78]. Several recent reviews have indicated the need for availability studies and speciation studies to better understand the mechanisms controlling P uptake and release from biochar [76,79,80]. Thus, the goal of this research is to test the potential of biochar and activated carbon to sorb P, identify speciation of the P on the biochar, and measure the subsequent P release behaviors.

Iron is an important chemical used in water treatment and can have lower life-cycle impacts compared to other metal salts often used for waste water treatment [81]. Since iron modification of biochar will increase P recovery potential, this research will test how Fe modification

affects P sorption and release. One biochar used in this study is a commercially available product produced from woody conifer forest biomass, the other is produced from anaerobically digested dairy waste biomass that is specifically designed to have enhanced P recovery properties [44]. Activated carbon was tested in this study since this is a standard water treatment substrate. While many studies create custom biochar to test properties and behaviors, in this study, a commercially available biochar was compared to a custom biochar to assess if a biochar produced using common manufacturing processes can be used in wastewater treatment plants to recover P. Sorption isotherm experiments were done to measure the amount of P that the unmodified and modified biochars sorb. Phosphorus release behaviors from the different biochars and activated carbon were characterized using stirred-flow reactor experiments, which simulates P release behavior in soils caused by either leaching or plant uptake. To support mechanistic understanding of sorption and release processes, X-ray spectroscopy was used to investigate P speciation on the biochars and activated carbon.

2. Methods

2.1 Biochar and activated carbon materials

Biochar and activated carbon production details are listed in Table 1. The AD biochar was added since it is a modified biochar designed for optimal P sorption and is thus a state-of-the-art biochar material for comparison to the commercially available pine feedstock biochar (BN). The activated carbon (AC) is a specially produced for water purification (product PSC325, particle size < 325 microns, certified by NSF-61 and AWWA-B600). The BN was sieved to a particle size of 850–150 μm. The AD Biochar was used as received (less than 850-μm fraction).

2.2 Iron-modified biochar preparation

To modify the biochars and AC, concentrated $FeCl_3$ solution was acquired from Kemira Inc. (Helsinki, Finland) (product PIX-311, which is a water treatment chemical; 39.8% w/w Fe concentration). For modification, 15 g biochar or AC was suspended in ~500 ml of 18 mΩ ultrapure water. The solution was stirred for 10 min at 700 rpm using a magnetic stir bar, after which 1M HCl was added dropwise until the suspension reached a pH of ~ 3.5–4. After the pH was stable, $FeCl_3$ was added to the suspension to create Fe weight percents from 0.5% to 8%; in this paper the focus is on the 2% Fe-modified biochar because it showed maximum increase in P sorption per Fe addition. The modification suspension was reacted for ~15 min and then titrated with 1.0 and 0.1 M NaOH to achieve a final pH of 6.5. Care was taken to slowly bring the solution up to the final pH to promote Fe sorption on the biochar particles as opposed to formation of a separate solid phase. After 10 min of stable pH, the suspension was centrifuged at 3000 relative centrifugal force for 10 min. The sedimented biochar or AC were then resuspended twice in 200 ml of 18 mΩ ultrapure water followed by another centrifugation and

Table 1. Biochar source and production.

Biochar	Feedstock	Production details	Source
Biochar Now (BN) (acquired 2019)	Lodgepole pine forests, western USA	Pyrolyzed at 550˚C to 650˚C	Biochar Now, LLC (Loveland CO, USA)
Anaerobic digest (AD)	Dairy manure anaerobic digest	Pyrolyzed at 750˚C under ammonia gas (detailed in Mood *et al.* [44]	Professor M. Garcia-Perez, Washington State University, (Washington, USA)
Activated carbon (acquired 2019)	Coconut shells	Pyrolyzed at 500˚C to 600˚C; steam at 800˚C to 1100˚C; optimized for use in water treatment [82]	Karbonous Inc. (California, USA)

https://doi.org/10.1371/journal.pwat.0000092.t001

separation. The modified biochar and AC were air dried for 72 h. The non-modified biochar was also rinsed three times to make it comparable to the Fe-modified biochar.

2.3 Biochar characterization

Biochars were digested with a modified dry ash method as described by Enders *et al.* [83]. Briefly, 200 mg of air-dried sample was added to ceramic crucibles, placed in a muffle furnace, and slowly heated to 500˚C for 10 h. The ash was transferred to plastic digestion tubes and digested twice with concentrated HNO_3 at 120˚C to dryness. Next, 1.0 ml trace metal grade HNO_3 and 4.0 ml reagent grade 30% H_2O_2 was added, and the tubes were placed back in the pre-heated block and processed at 120˚C to dryness. The residue was solubilized with 1.4 ml of concentrated HNO_3 and 48.6 ml 18 Ωm water. Samples were vortexed for 1 min and filtered through a 0.45 μm PES syringe filter (Tisch Scientific, Cleves, OH). Samples were analyzed by ICP spectrometer for elemental composition using certified standards (SPEX CertiPrep (Metuchen, NJ USA)). Duplicates were run in all digestion batches and were within 10% of each other. For CNS analysis, samples were air-dried for 72 hours, ground to pass a 250-μm sieve and oven dried for 24 hrs at 65˚C.

Biochar and AC samples were analyzed for total carbon, nitrogen, and sulfur on an Elementar vario Max cube (Elementar Americas Inc., Ronkonkoma, NY, USA). pH and electrical conductivity were measured on a 1:10 solid to solution slurry.

2.4 Phosphorus sorption isotherms

Phosphorus sorption behavior on the biochars was measured using isotherm methods described in Graetz *et al.* [84]. Briefly, a 1000 mg/L P stock solution was prepared with $Na_2HPO_4 \cdot 7H_2O$ (Fisher Scientific Inc., Massachusetts, USA) diluted to 100, 75, 50, 20, 10, 5, 2, 1, and 0.5 mg/L P. The pH of the solutions was adjusted to 6.5 with 0.1 and 0.01 M HCl. In this study we chose pH 6.5 because it is a near neutral pH, reflecting the pH of many wastewaters, and because P adsorption on iron oxides is relatively high at that pH and decreases as pH increases [85]. 0.2 g of rinsed biochar or AC for each concentration was placed in 15 ml polypropylene centrifuge tubes. Each sample concentration was run in triplicate. 5.0 ml of 18 mΩ ultra-pure water was added to each tube. The suspensions were allowed to equilibrate for ~30 minutes, then the pH checked again and adjusted to 6.5. The appropriate volume of stock solution was then added to the pH adjusted slurry. The remaining volume of water was added to bring the total solution volume to 10 ml, yielding a 1:50 solid to solution ratio. The tubes were placed on an end-over-end shaker and reacted at lab temperature ~22˚C for 24 hours at 30 rpm. Post-incubation samples were allowed to settle for ~30 min and a final pH was measured. The samples were centrifuged at 3000 relative centrifugal force for 10 min, and supernatant was syringe filtered through a 0.45 μm PES filter. Solutions were analyzed by either molybdate blue colorimetric assay for dissolved reactive phosphorus [86], or by ICP-AES as described above. The molybdate blue reagent was prepared as outlined by Pote *et al.* [87]. Solutions were analyzed on a GENESYS 10S UV-VIS Spectrophotometer (Thermo Scientific, Waltham, MA) at 880 nm wavelength.

The amount of P sorbed (Q) on the biochars and AC was calculated using the following equation:

$$Q = (C_i - C_e) \times (V/m)$$

Where Q is phosphorus adsorbed (mg/kg); C_i is initial P concentration (mg/L); C_e is equilibrium concentration (mg/L); V = volume of solution (L); m = mass of biochar (kg). The adsorption isotherms were fit using Freundlich and Langmuir adsorption isotherm models [88],

implemented as nonlinear fit optimization algorithms in the software OriginLab (Northampton, MA, USA).

2.5 Phosphorus release

Phosphorus release studies were done on biochar and AC that had no P addition, and biochars incubated in 10 mg/L P solution using the same procedure described in the isotherm experiments. The release studies were done by leaching DI water adjusted to pH 6.5 through a polycarbonate stir-flow cell [89] with a peristaltic pump at 2.0 ml min^{-1}. The stirred-flow cell was fitted with a 0.45 μm PES filter. The effluent was collected in 6.0 ml increments in a fraction collector. The pH of the effluent was periodically checked in the collection tubes. Solutions were analyzed on the ICP-AES or colorimetric analysis as previously described. Release data are plotted as percent P release as a function of the volume of effluent. Percent P released per volume effluent was calculated as the area of the release concentration curve, summed for each time interval, divided by the total amount of P on the biochar as determined by digestion.

2.6 Phosphorus K-edge XANES analysis methods

X-ray absorption near edge structure (XANES) spectroscopy was used to determine P species present in biochar and AC samples. All samples were ground and sieved to less than 500 μm before mounting to a sample holder. P K-edge XANES spectra of biochars and AC were collected at the Canadian Light Source (CLS) on the Soft X-ray Micro-Characterization Beamline (SXRMB). SXRMB uses an InSb(III) monochromator with a 300 μm x 300 μm beam. The beamline was calibrated to 2158 eV using $ZnPO_4$ powder. Spectra were collected from 2135–2190 eV with a step size of 1 eV on the pre-edge region (2110–2145 eV), 0.25 eV in the near edge region (2145.25–2180 eV), and 0.5 eV in the post edge region (2180.5–2200 eV). Multiple spectra were collected for each sample.

The collected scans were analyzed using the Athena software program [90]. Replicate spectra from each sample were averaged. Each spectrum was calibrated at 2151.6 eV set as the inflection point of the main edge, allowing for the main edge peak height and shape, and pre-edge or post-edge peaks to be linearly separable elements in linear combination fitting (LCF). The same background subtraction parameters were used for each spectrum to provide consistent background subtraction effects across the samples and standards. Supervised linear combination fitting was performed to determine the speciation of each spectrum. Initially, all standards were used to fit the spectra, followed by a reduction to five standards that were deemed to represent the major species possible in the sample spectra (adsorbed P, apatite, dicalcium phosphate dihydrate (DCPD), DCDP with 50:50 Ca to Mg ratio, and phytic acid as an organic P standard). Standards were iteratively removed if they comprised zero or negative contributions to the sample fit. The fits were not forced to sum to 100% but were checked to ensure that all fits were within 10% of 100%, which is an important criterion for evaluating normalization effects. Accuracy of LCF has been estimated to be between 5% to 15% percent absolute in the sample and standard sets that are carefully calibrated and screened to reduce data collection and processing artifacts [91,92], and likely higher when these artifacts are less well controlled. In fitting of the spectra, it was observed that in some spectra, Ca-P minerals could be substituted for each other with only a slightly decreased fit quality as judged by reduced chi-square. However, in no cases could the Ca-P minerals be eliminated or replaced with another component in a fit. Thus, the fit of these mineral standards is grouped as Ca-P minerals instead of individual Ca-P species.

Table 2. Chemical properties of biochar and activated carbon.

Name	EC (μs/cm)	pH	Volatile (%)	Ash (%)	Fixed C (%)	C (%)	N (%)	Ca (mg/kg)	Fe (mg/kg)	Mg (mg/kg)	Mn (mg/kg)	P (mg/kg)	Formic Acid Extractable (mg/kg)
Biochar Now	190	9.6	15.1	29.0	55.8	70.3	0.6	10500	7400	1910	211	315	150
Anaerobic Digested Fiber	3550	11.6	21.7	28.3	50.0	51.4	10.2	49700	2840	18600	397	16500	14800
Powdered Activated Carbon	512	9.8	9.12	14.0	76.9	78.7	0.1	20150	6540	4780	612	1020	710

https://doi.org/10.1371/journal.pwat.0000092.t002

2.7 SEM analysis of biochar

Scanning electron microscopy (SEM) and X-ray fluorescence analysis of the BN biochar samples were done using a Zeiss Supra 35 FEG-SEM. AD biochar SEM was previously reported in Mood *et al.* [44]. Biochar samples were mounted on a metal stub and carbon coated and analyzed at an accelerating voltage of 20 kV.

3. Results and discussion

3.1 Biochar characterization

The pH of the biochar and activated carbon are alkaline (Table 2), likely due to the presence of carbonate minerals and alkali salts [93]. The pH of the Fe-modified AD, BN, and AC samples were 8.19, 6.98 and 6.51, respectively. The Fe modification process treats the biochar in an acidic suspension followed by base addition to increase the pH to 6.5, which should dissolve and rinse out many of the salts and carbonates that create alkaline biochar solutions; however, the amount of carbonates removed may vary depending on the mineral size and reactivity. The decreased pH may impact soil solution chemistry when the Fe-modified biochars are amended to soils.

Total P in the biochar and AC samples ranged from 314 mg/kg in the BN sample to 16,500 mg/kg in the AD sample (Table 2). Feedstock is the major factor controlling total P. Phosphorus content of plants is variable, and in wood from pine trees (feedstock for the BN biochar), total P may be as low as 100 mg/kg [94]. The AD biochar created from anaerobically digested cow manure has the highest P content due to the high P concentration in the cow manure feedstock.

Plant available P from the biochar and activated carbon samples was assessed using the formic acid leachable P test [95]. The P in the AD biochar sample was 90% plant available. In the BN biochar and AC samples, P was 48% and 69% available, respectively. Thus, the availability of the biochars' native P is variable, depending on feedstock and production methods, which has been observed in many studies on plant uptake of P from biochar [28,29]. Other element compositions are also reported in Table 2, including N, which is an important macronutrient, and Fe, Ca, and Mg, which are important nutrients for plants and are also reactive components of biochar that promote P sorption.

SEM images of the BN biochar showed some mineral grains of silicates and calcium carbonates amongst the biochar particles (S4 Fig). SEM analysis of the AD biochar by Mood *et al.* [44] showed the presence of small clusters of Mg and Ca minerals dispersed on the surface of the biochars. SEM images from the Fe-modified biochars did not show any Fe mineral particles, only slightly enriched Fe biochar particle regions (S4 Fig), suggesting the Fe is precipitated or sorbed on the biochar surfaces.

3.2 P sorption behavior

Phosphate sorption behavior on the biochars and activated carbon showed high relative amounts of sorption at low concentrations, followed by decreased sorption as concentration increased (Fig 1). The sorption isotherms on BN and AD biochars and the AC sample show typical sorption behavior that occurs when there is a high affinity for sorption, but sorption sites are limited and become saturated as solution P concentration increases [96]. If phosphate removal was dominated by a bulk precipitation process, the sorption isotherm would continuously increase as solution concentration increases, dictated by the solubility of a solid. The isotherm data on the BN biochar (Fig 1C) and the AC (Fig 1A) were fit using the Freundlich isotherm model equations (S1 Table); the Langmuir isotherm model was a poor fit to the data on these samples. On the AD biochar (Fig 1B), the Langmuir isotherm model fit the sorption data slightly better than the Freundlich model, although both fits were good. While both the Freundlich and Langmuir isotherm equations fit non-linear adsorption trends with steep initial slopes, the Langmuir isotherm equation fit provides a sorption maximum value, while the Freundlich isotherm equation does not predict a maximum sorption amount but fits a logarithmic growth sorption curve [97]. Sorption isotherms are useful for predicting concentrations of sorbate at a particular solution concentration, however, interpreting mechanistic reaction processes from the isotherm fit parameters is not possible [98].

After Fe modification, P sorption increased in the BN biochar and AC sample (Fig 1C); P sorption maximum in 2% Fe-modified BN biochar increased by nearly 10 times more than the unmodified BN biochar. The untreated AC had a high P sorption capacity and modifying with 2% Fe increased the sorption capacity by ~30% (Fig 1A), which is a much smaller percent increase than observed in the BN biochar.

The unmodified AD biochar had the highest P sorption capacity of all biochars tested in this study, and when it was modified with Fe, P sorption capacity decreased (Fig 1B). Phosphorus sorption behavior of the AD biochar was studied by Mood *et al.* [44]. They reported that the P sorption capacity was three orders of magnitude greater than observed in this study, however, the incubation pH used in their study was much higher (pH = 10) than this study (pH = 6.5). At higher pH, the solution will be supersaturated with respect to Mg-P and Ca-P minerals, and the P sorption is not limited by surface properties, and thus greater P removal from solution occurs because of mineral precipitation. SEM and X-ray photoemission spectroscopy (XPS) analysis by Mood *et al.* [44] confirmed the presence of Ca-P minerals. At pH 6.5, phosphate bonding to the positively charged amine functional groups on the AD biochar may be a dominant sorption mechanism in addition to possible Ca or Mg phosphate mineral precipitation. Modifying the AD biochar with 0.5% Fe may have blocked access to the amine functional groups, thus decreasing sorption capacity (Fig 1B). Increasing the Fe modification of the AD biochar from 0.5 to 2% Fe, the sorption capacity increased, but it still did not surpass the P sorption capacity of the unmodified AD biochar. This is likely due to the blocking of the amine functional groups that is countered by addition of more iron-phosphorus adsorption sites than occurred in the 0.5% Fe-modified AD biochar.

Research on biochars made from traditional carbon-rich biomass feedstock such as forest biomass, plant fibers from agricultural residue, and coconut fibers, indicates that they do not sorb large amounts of P. Several papers have provided methods for modifying the biochars to enhance P sorption [15]. Some of the most common modifications include adding Fe to the biochar [50,52,55] or adding Ca or Mg [60,63,64]. Other more complex modification methods have also been developed to produce magnetic biochars [68–70] as well as the AD biochar that was modified by pyrolyzing anaerobic digestate in the presence of ammonia gas to create positively charged amine functional groups that can adsorb P [44]. Iron modification is often

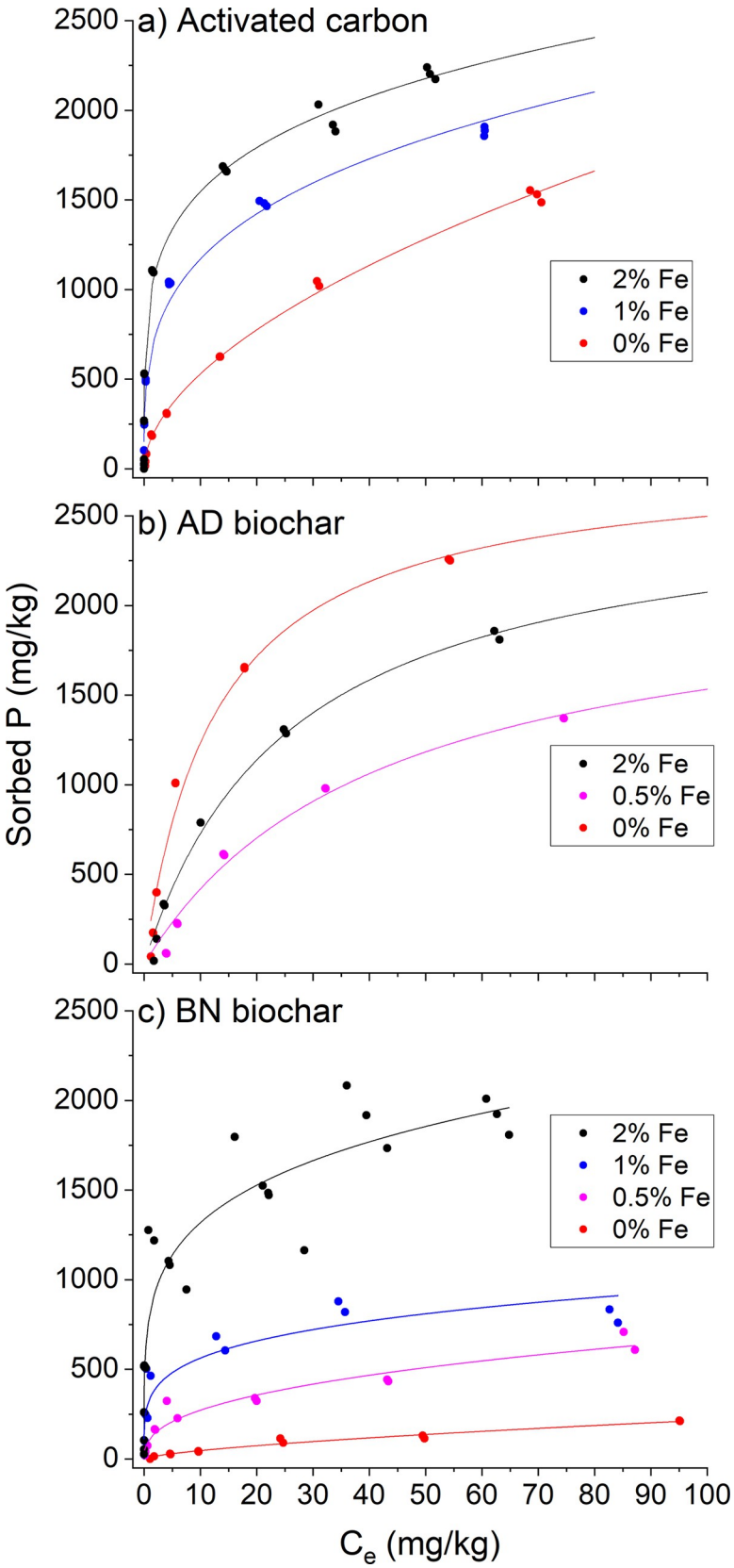

Fig 1. Sorption isotherms of phosphorus on unmodified and modified biochar. Solid lines are fits of isotherms using either the Langmuir (AD) or Freundlich (BN and AC biochar) models (Fit parameters are reported in S1 Table).

https://doi.org/10.1371/journal.pwat.0000092.g001

proposed because it is an inexpensive method to increase P adsorption on biochars; additionally, the addition of Fe may be beneficial as a soil amendment on the P-loaded biochar. Results from the P sorption isotherm studies show that Fe modification enhances P sorption on biochar or activated carbon made from woody biomass (AC (Fig 1A) and BN (Fig 1C)), but that more specialized biochars, like the AD biochar (Fig 1B), may not need post-production iron modification. The enhanced P sorption on Fe-modified biochars provides a method for recovering P from waste waters and supports creating an enhanced efficiency P fertilizer needed to support a circular bioeconomy that includes P recycling [12,15,16].

3.3 Phosphorus K-edge XANES spectra

Phosphorus K-edge XANES spectra from the biochars and activated carbon are shown in Fig 2 and fit results are reported in S3 Table. Linear combination fitting of P XANES has a fair amount of uncertainty because of the lack of differences in spectral features between molecular species and spectral artifacts that may cause errors in the LCF results [91,99–101]. This uncertainty is especially problematic in natural samples because the standard set may be missing species that are present in the sample, but the fit can still have good fit statistics [101,102]. The standards used in fitting the biochar and activated carbons are shown in S3 Fig. For some species, there are distinguishing features that can be used for species identification, such as the post-edge shoulder at 2155 eV in the spectra of the Ca-P minerals. While other species are distinguished only by the intensity of the main-edge peak. Because the biochar and AC sample spectra are comprised of several species, the LCF results are used to categorize the P as either Ca-P or adsorbed/organic P rather than assigning specific species. In all but one sample, either hydroxyapatite or DCPD were fit as one of the species present that were categorized as Ca-P minerals. Ca-P species fit results ranged from 28% to 83% of the total P species in the biochar samples (S3 Table).

The P K-edge XANES spectra from the biochar and activated carbon samples are shown in Fig 2. There are distinct differences between the untreated and Fe-modified samples, especially in the post-edge shoulder at 2155 eV and the small peak at 2163 eV. Both features are indicative of Ca-P minerals; these peaks are most prominent in hydroxyapatite (S1 Fig). The unmodified BN, AD and AC samples all had strong Ca-P minerals peaks. Despite the uncertainty in LCF of P in natural samples, these peaks are distinctive, and their presence clearly shows that Ca-P minerals are a major species occurring in the biochars. The AC and BN samples had the most Ca-P mineral present in the LCF results (82%, S3 Table). Calcium phosphate minerals, like hydroxyapatite, have low solubility [103,104]. Thus, it is anticipated that P release from these biochars would be less than P sorbed on mineral surfaces [105,106]. The occurrence of P in Ca-P species in biochar is likely a result of the presence of Ca in the ash, which comes from Ca in the biomass feedstock. The Ca in the feedstock can either be plant-based Ca that gets released during pyrolysis (Ca is a significant element of biological tissues), or as mineral dust in the biomass feedstock taken in from soil attached to the biomass feedstock or mixed in with the biomass when it is collected from the environment during harvesting.

The P K-edge XANES spectra from the Fe-modified AD and BN biochars and the AC sample all show decreased peak intensity for the Ca-P peaks at 2155 eV and 2163 eV compared to the non-Fe modified samples (Fig 2). In the AC sample, there is nearly a complete loss of the Ca-P mineral features in the spectrum after Fe modification. The LCF results of the AC samples show that the Ca-P mineral species decreased from 82% in the unmodified AC sample to only 28% in the Fe-modified AC sample, indicating a major shift in species to P sorption on iron oxides in the Fe-modified AC sample. Possible sorption mechanisms for P on the Fe-modified biochar are: 1) ternary biochar-Fe-P complexes similar to how P adsorbs on natural

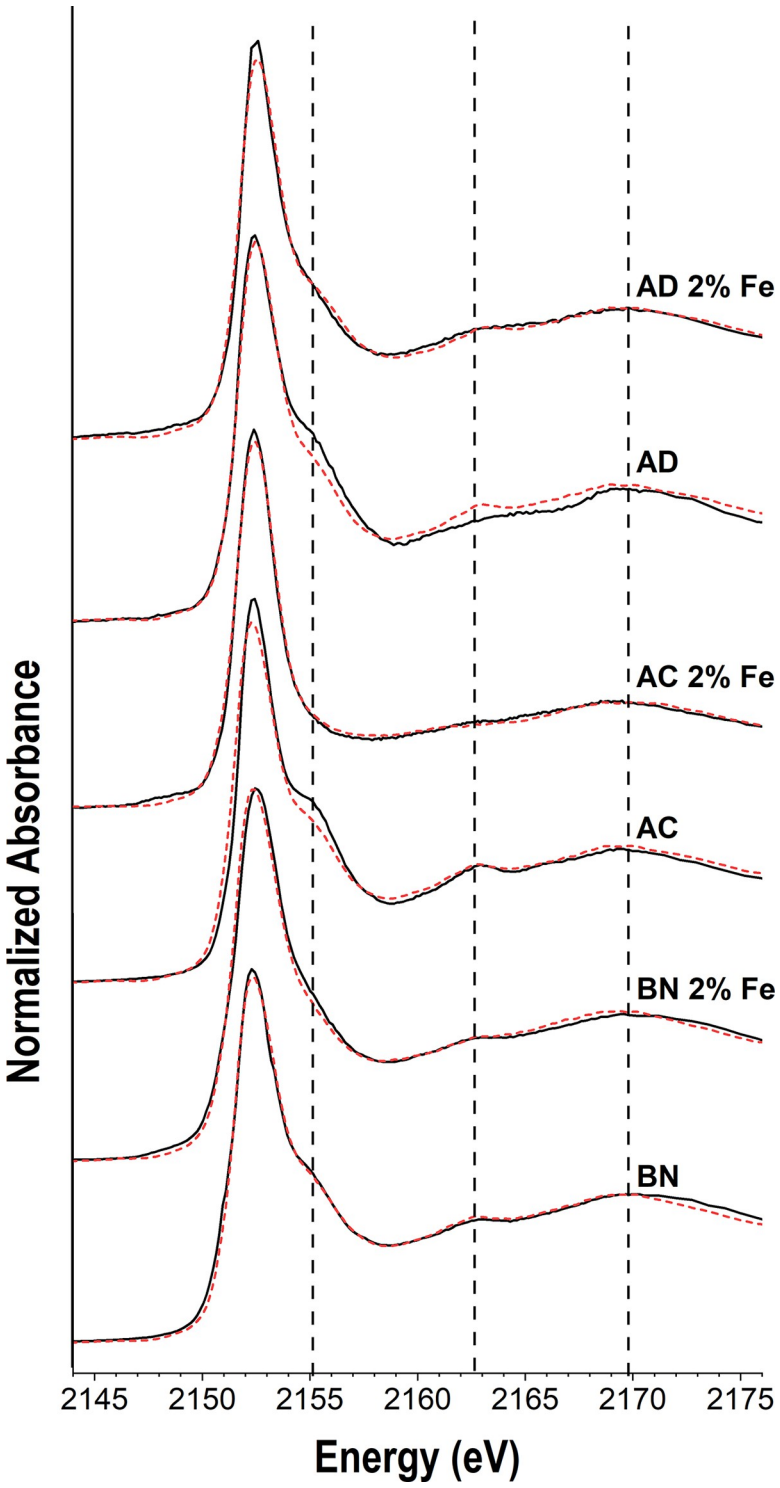

Fig 2. Phosphorus K-edge XANES spectra (solid lines) from biochar and activated carbon samples, and best fits from LCF using standards (dashed lines). Fit results are reported in S3 Table. Vertical lines indicate distinctive XANES spectral features.

https://doi.org/10.1371/journal.pwat.0000092.g002

organic matter [16,107]; 2) phosphate adsorption on iron oxide phases that may exist either on the surfaces of the biochar as surface precipitates; or 3) P sorption on small, possibly nano-sized, precipitates co-mingled with the biochar. Fe-modified BN and AD biochar also had a decrease in Ca-P species in them, as indicated by the decrease in the peaks at 2155 eV and 2163 eV, suggesting that P is sorbing on the Fe phases on the biochar in these samples.

3.4 P release behavior

Recovery of P on biochar creates a pathway for nutrient recycling when the biochar is used as a soil amendment and may promote additional soil health benefits [30,77], such as increasing soil carbon, providing required nutrients, and promoting soil structure that allows better water retention, root development and gas exchange. Phosphorus in soils is not typically readily available because it strongly bonds to iron and aluminum oxides in acidic soils and forms calcium phosphate minerals in alkaline soils [108]. Thus, P release from the Fe-modified biochar needs to be measured to understand how much of it is available for plant uptake.

The percentage of total P released from the different biochars and activated carbon are shown in Fig 3A and 3B (total P is listed in Tables 2 and S2). An important factor in P sorption and release behavior is solution pH. The influent solution pH was adjusted to 6.5 in these experiments, however, the effluent pHs were different: AC sample pHs ranged from 8.8–9.5; Fe-modified AC pHs ranged from 4.5–4.8; BN sample pHs ranged from 9.3–9.4; Fe-modified BN pHs ranged from 6.1–6.8; AD sample pHs ranged from 6.9–9.2; and Fe-modified AD sample pHs ranged from 4.6–7.1. In all Fe-treated biochar samples, the effluent pHs were 2–3 units lower than they were in the untreated samples. This occurs because the Fe-modification procedure used an acidic Fe solution to incubate the biochars before titrating the suspensions to pH 6.5, which leached out many of the alkaline salts and carbonate minerals. Additionally, the release of phosphate adsorbed on iron oxides is a ligand exchange reaction, thus consuming hydroxide ions and decreasing pH. The varying pH of the biochar and AC samples is an important factor in the behavior of the P release curves. The change in effluent pH in the stirred-flow reactor simulates the effects that would occur in biochar-amended soils when P desorbs and leaches out of the soils into surface or groundwaters.

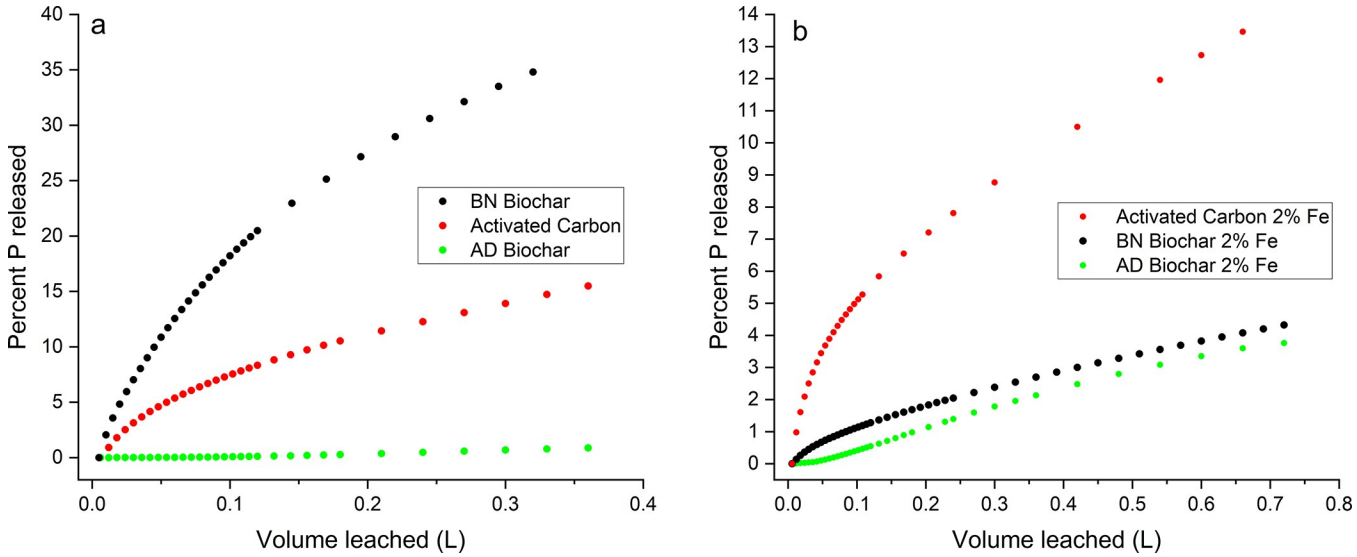

Fig 3. Percent P released into solution from unmodified (panel a) and Fe-modified (panel b) biochars and activated carbon. Fe-modified chars were incubated in a 10 mg/L P solution prior to the stirred-flow reactor leaching experiments (P loading reported in S2 Table).

https://doi.org/10.1371/journal.pwat.0000092.g003

The unmodified BN biochar released the most P (Fig 3A); ~35% of the total P was released after 0.35 L of leaching, and the positive slope at the end of the experiment suggests P release will continue with more leaching. The AD biochar released very little P (<1% of its total P), indicating that the P is strongly bound in the AD biochar as a poorly soluble species. Phosphorus release from the AC sample was only about 13% of total P after 0.35 L, but even after 0.35 L of leaching, the slope remains positive, suggesting that P leaching will continue. The P species in the AC sample may be a low solubility species that has slow release.

The percentage of P released from the Fe-modified BN biochar and AC sample (Fig 3B) were much less than in the unmodified samples (Fig 3A). Iron-modified AD biochar released slightly more P (~4% after 0.7 L) compared to the unmodified AD biochar (<1%). The greatest amount of P release was from the Fe-modified AC sample, which released ~14% of the P after ~0.7 L of leaching, and the steep slope indicates that additional leaching will release more P. The Fe-modified BN and AD biochar samples both released ~4% of the sorbed P after 0.7 L, and the slope also suggests that P release will continue. The continuous P release in the Fe-modified samples suggests that their use as a slow release fertilizer is promising. However, complete assessment of P availability would require a plant growth trial since plant rhizosphere reactions may enhance P mobility by release of low molecular weight organic acids [109].

Release of Ca and Mg cations during the stirred-flow experiments was also measured (S1 and S2 Figs). Initially, Ca and Mg concentrations were high in all the biochar leaching experiments, followed by a tailing off to a constant low concentration. There are direct relationships between Ca concentrations and P release in the AC sample and AD biochar, which likely reflects the solubility control from calcium phosphate minerals. The Mg release in the AD biochar was inhibited until Ca concentrations decreased. It has been observed that the presence of Mg inhibits apatite formation, favoring meta-stable Ca-P minerals because of the isomorphic substitution of Mg for Ca [110]. Upon Fe amendment, P release was not related to Ca and Mg in the BN and AD biochars. However, there remained a significant inhibition of P release concentration in the AC sample when the Ca and Mg concentrations were high (S2 Fig).

Amongst the Fe-modified samples, the Fe-modified AC sample had the most P release in the stirred flow experiments (Fig 3B), which corresponds to the XANES spectra results showing it had the biggest decrease in the poorly soluble Ca-P minerals. While sorbed P is more available for release to solution than many Ca-P species, its desorbability should still be low [111]. The release curves of P from the Fe-modified BN and AD samples were less than the Fe-modified AC sample. The XANES spectra showed that in the Fe-modified BN and AD samples there was still 37–65% Ca-P minerals (S3 Table), which is more than remained in the Fe-modified AC sample (28% Ca-P species, decreased from 83% in the non-Fe-modified AC sample).

3.5 Phosphorus sorption and release mechanisms

The highest phosphorus sorption capacity by unmodified biochars occurred on the AD biochar produced from anaerobic digest solid separates under ammonia gas pyrolysis. This biochar has positively charged amine functional groups that can adsorb the phosphate anions, thus facilitating a high sorption capacity [44]. However, the P XANES spectra from the AD biochar sample showed that the majority of P in this biochar exists as Ca-P mineral phases, which is in agreement with the findings of Mood *et al.* [44], who characterized the P sorption behavior of AD biochar at a higher equilibrium pH than used in this experiment.

Based on the P release experiments, the Ca-P species in the AD biochar are not soluble, which agrees with the expected solubility of Ca-P minerals such as hydroxyapatite [104]. In contrast, Kizito *et al.* [112] measured P sorption from anaerobically digested swine manure effluent onto biochars and observed that the sorbed P was completely reversible. Based on

sorption and molecular analysis, Kizito *et al.* [112] proposed that phosphate was precipitating as Ca-P minerals, which generally have low solubility when they exists in the most stable forms (i.e., hydroxyapatite). However, biochar produced from animal manures may have meta-stable Ca-P minerals that have higher solubility than the hydroxyapatite. The meta-stable Ca-P minerals are favored because high concentrations of Mg in the dairy manure may isomorphically substitute for Ca inhibiting hydroxyapatite formation [110], and also because dissolved organic matter inhibits hydroxyapatite formation [113,114]. These mechanisms could have inhibited the formation of the most stable Ca-P minerals in the biochar produced by Kizito *et al.* [112], but, due to differences in pyrolysis methods, may not have inhibited formation of more crystalline Ca-P minerals in the AD biochar, explaining why it had very low P release behavior. Iron modification decreased the amount of P sorption on the AD biochar, and P XANES indicated that more of the P in this sample existed as P sorbed as Fe-ternary complexes or sorbed on Fe-oxide nanoparticles on the biochar surface rather than Ca-P species. When Fe modified, the AD biochar released more P in the stirred-flow reactor compared to the unmodified AD biochar. Thus, this may be a suitable strategy to create a biochar that has both slow and fast release P for use as a soil amendment.

The BN biochar had low P sorption capacity, and Fe modification increased the sorption capacity. The most prominent P species in the BN biochar was a Ca-P species, which likely formed from the Ca released from Ca carbonates in the ash fraction of the sample. Iron modification of the BN biochar increased the amount of P-Fe-biochar ternary complexes. Phosphorus release concentrations from the Fe-modified BN sample were much less than in the unmodified BN sample.

Results from this study show that Ca-P minerals are common in biochar, likely due to the alkaline pH and high amounts of Ca salts in the ash contained within the biochar. Magnesium phosphate minerals may also be present in biochars, particularly in biochars with high Mg concentrations [41,53,58,59,64], such as the AD biochar sample. Although Ca-P minerals typically have low solubility, the solubility varies, depending on the crystallinity of the Ca-P species [103]. Thus, some Ca-P minerals may be soluble and would be a good P fertilizer in the biochar-amended soils.

4. Conclusion

Biochar can be used in water treatment to recover P for recycling as a beneficial soil amendment, however, modification with metals such as iron may be required to sufficiently increase the biochar P sorption capacity. Modification of biochar with Fe changes the P speciation on the biochar and thus will change the P release behavior and the potential biochar fertilizer properties. In a recent review, Nobaharan *et al.* [16] proposed several areas of research that are needed to realize the potential of biochar uses in wastewater treatment to promote P recycling. The suggestions included: 1) best practices for biochar modification to increase P recovery from wastewaters, 2) characterization of the P-enhanced biochar to understand P sorption mechanisms, and 3) determination of P release from the P-loaded biochar. Results from the research presented in this paper address these research needs, providing fundamental information needed to advance P-biochar sustainability. However, to accurately evaluate the potential of P-loaded biochar to supply P for plant uptake, plant growth studies in amended soils is needed since root rhizosphere processes alter the chemistry of the soil solution and thus P bioavailability [109]. Additionally, since organic contaminants in wastewater may pass through the primary and secondary treatment (e.g., perfluoroalkyl and polyfluoroalkyl substances (PFAS)) and are known to adsorb on activated carbon and biochar [115], the effects of Fe modification on this process and potential impacts and risks of transferring these

contaminants to soil needs to be addressed. Despite these challenges, using biochar to recover P is a promising technology for sustainable P use that can support a carbon negative water treatment process.

Supporting information

S1 Fig. Concentrations of Ca, Mg, and P released form AD biochars in stirred flow release experiments.
(DOCX)

S2 Fig. Concentrations of Ca, Mg, and P released form BN biochar and activated in stirred flow release experiments.
(DOCX)

S3 Fig. Near-edge XANES spectra from various phosphorus standards. Standards abbreviations are as follows (DCDP = dicalcium phosphate dihydrate; DCDP50:50 Ca:Mg = Mg and Ca mixed DCDP; Fe-P = strengite; Al-P is AlPO4 from Werner et al. (99); Adsorbed P is P adsorbed on goethite at pH 6.5). The features of note are a pre-edge peak on Fe-phosphate (arrow), the main peak shape and intensity, the energy of the post-white line peaks near 2,155 eV, 2,163 eV and 2,169 eV (vertical dashed lines).
(DOCX)

S4 Fig. SEM images and EDS from BN biochar.
(DOCX)

S1 Table. Adsorption isotherm model fits for biochar and activated carbon P sorption data. Fits are shown in Fig 1 (AD biochar Freundlich fits not shown).
(DOCX)

S2 Table. Phosphorus loading on biochar and activated carbon used in release experiments and on samples used for XAFS analysis.
(DOCX)

S3 Table. Fit results of LCF of P XANES.
(DOCX)

Acknowledgments

Parts of the research described in this work were performed at the Canadian Light Source. The Canadian Light Source is supported by the Canada Foundation for Innovation, Natural Sciences and Engineering Research Council of Canada, the University of Saskatchewan, the Government of Saskatchewan, Western Economic Diversification Canada, the National Research Council Canada, and the Canadian Institutes of Health Research. We thank Solana Narum, Martin Baker, and Mike Vogler for assistance in laboratory research, and Tom Williams for assistance with SEM analysis.

Author Contributions

Conceptualization: Daniel G. Strawn, Manuel Garcia-Perez, Gregory Möller.

Data curation: Daniel G. Strawn, Alex R. Crump, Derek Peak.

Formal analysis: Daniel G. Strawn, Gregory Möller.

Funding acquisition: Daniel G. Strawn, Gregory Möller.

Investigation: Daniel G. Strawn, Alex R. Crump, Derek Peak.

Methodology: Daniel G. Strawn, Alex R. Crump, Derek Peak, Manuel Garcia-Perez.

Project administration: Gregory Möller.

Resources: Manuel Garcia-Perez.

Visualization: Daniel G. Strawn.

Writing – original draft: Daniel G. Strawn.

Writing – review & editing: Daniel G. Strawn, Alex R. Crump, Derek Peak, Manuel Garcia-Perez, Gregory Möller.

References

1. Jupp AR, Beijer S, Narain GC, Schipper W, Slootweg JC. Phosphorus recovery and recycling–closing the loop. Chem. Soc. Rev. 2021; 50(1):87–101. https://doi.org/10.1039/d0cs01150a PMID: 33210686
2. Carey R, Migliaccio K. Contribution of wastewater treatment plant effluents to nutrient dynamics in aquatic systems: A review. Environ. Manage. 2009; 44:205–17. https://doi.org/10.1007/s00267-009-9309-5 PMID: 19458999
3. Cordell D, Neset TSS. Phosphorus vulnerability: A qualitative framework for assessing the vulnerability of national and regional food systems to the multi-dimensional stressors of phosphorus scarcity. Global Environ Change. 2014; 24:108–22.
4. Shepherd JG, Sohi SP, Heal KV. Optimising the recovery and re-use of phosphorus from wastewater effluent for sustainable fertiliser development. Water Res. 2016; 94:155–65. https://doi.org/10.1016/j.watres.2016.02.038 PMID: 26945452
5. Shaw A, Barnard J. What is your phosphorus footprint? Proc. Water Env. Fed. 2011;(12):4422–9.
6. de Ridder M, de Jong S, Polchar J, Lingemann S. Risks and Opportunities in the Global Phosphate Rock Market. Netherlands: The Hague Centre for Strategic Studies (HCSS), 2012 17, 12, 12.
7. Elser JJ. Phosphorus: A limiting nutrient for humanity? Curr. Opin. Biotech. 2012; 23(6):833–8. https://doi.org/10.1016/j.copbio.2012.03.001 PMID: 22465489
8. Wilfert P, Kumar PS, Korving L, Witkamp GJ, van Loosdrecht MCM. The relevance of phosphorus and iron chemistry to the recovery of phosphorus from wastewater: A review. Environ Sci. Technol. 2015; 49(16):9400–14. https://doi.org/10.1021/acs.est.5b00150 PMID: 25950504
9. Newcombe RL, Strawn DG, Grant TM, Childers SE, Moller G. Phosphorus removal from municipal wastewater by hydrous ferric oxide reactive filtration and coupled chemically enhanced secondary treatment: Part II—Mechanism. Water Environ. Res. 2008; 80(3):248–56. https://doi.org/10.2175/106143007x220987 PMID: 18419013
10. Newcombe RL, Rule RA, Hart BK, Moller G. Phosphorus removal from municipal wastewater by hydrous ferric oxide reactive filtration and coupled chemically enhanced secondary treatment: Part I—Performance. Water Environ. Res. 2008; 80(3):238–47. https://doi.org/10.2175/106143007x221003 PMID: 18419012
11. Newcombe RL, Hart BK, Moller G. Arsenic removal from water by moving bed active filtration. J. Environ. Eng.-ASCE. 2006; 132(1):5–12.
12. Zamparas M, Kapsalis V, Kanteraki A, Vardoulakis E, Kyriakopoulos G, Drosos M, et al. Novel composite materials as P-adsorption agents and their potential application as fertilizers. Global NEST J. 2019; 21:48–57.
13. Tarragó E, Sciarria TP, Ruscalleda M, Colprim J, Balaguer MD, Adani F, et al. Effect of suspended solids and its role on struvite formation from digested manure. J. Chem. Technol. Biotechnol 2018; 93 (9):2758–65.
14. Kataki S, Baruah DC. Prospects and Issues of Phosphorus Recovery as Struvite from Waste Streams. In: Hussain CM, editor. Handbook of Environmental Materials Management. Cham: Springer International Publishing; 2018. p. 1–50.
15. Li SM, Chan CY, Sharbatmaleki M, Trejo H, Delagah S. Engineered biochar production and its potential benefits in a closed-loop water-reuse agriculture system. Water. 2020; 12(10).
16. Nobaharan K, Bagheri Novair S, Asgari Lajayer B, van Hullebusch ED. Phosphorus removal from wastewater: The potential use of biochar and the key controlling factors. Water. 2021; 13(4):517. P.

17. Wang X, Guo Z, Hu Z, Zhang J. Recent advances in biochar application for water and wastewater treatment: a review. PeerJ. 2020; 8:e9164–e. https://doi.org/10.7717/peerj.9164 PMID: 32477836

18. Xiang W, Zhang XY, Chen JJ, Zou WX, He F, Hu X, et al. Biochar technology in wastewater treatment: A critical review. Chemosphere. 2020; 252. https://doi.org/10.1016/j.chemosphere.2020.126539 PMID: 32220719

19. Mohan D, Pittman CU, Misna TE, editors. Sustainable Biochar for Water and Wastewater Treatment: Elsevier; 2022.

20. He XM, Zhang T, Ren HQ, Li GX, Ding LL, Pawlowski L. Phosphorus recovery from biogas slurry by ultrasound/H_2O_2 digestion coupled with HFO/biochar adsorption process. Waste Manage. 2017; 60:219–29.

21. Zhang T, Xu H, Li H, He X, Shi Y, Kruse A. Microwave digestion-assisted HFO/biochar adsorption to recover phosphorus from swine manure. Sci. Total Environ. 2018; 621:1512–26. https://doi.org/10.1016/j.scitotenv.2017.10.077 PMID: 29102181

22. Finn M, Rodriguez R, Contrino D, Swenson J, Mazyck DW, Suau S. Impact of inherent magnesium in biochar for phosphate removal from reclaimed water streams. J. Environ. Eng. 2022; 148 (2):04021085.

23. Yao Y, Gao B, Chen J, Yang L. Engineered biochar reclaiming phosphate from aqueous solutions: Mechanisms and potential application as a slow-release fertilizer. Environ. Sci. Technol. 2013; 47 (15):8700–8. https://doi.org/10.1021/es4012977 PMID: 23848524

24. Hagemann N, Joseph S, Schmidt HP, Kammann CI, Harter J, Borch T, et al. Organic coating on biochar explains its nutrient retention and stimulation of soil fertility. Nat. Commun. 2017; 8. https://doi.org/10.1038/s41467-017-01123-0 PMID: 29057875

25. Wang T, Camps-Arbestain M, Hedley M. The fate of phosphorus of ash-rich biochars in a soil-plant system. Plant Soil. 2014; 375(1–2):61–74.

26. Ghezzehei TA, Sarkhot DV, Berhe AA. Biochar can be used to capture essential nutrients from dairy wastewater and improve soil physico-chemical properties. Solid Earth. 2014; 5(2):953–62.

27. Dai YJ, Wang WS, Lu L, Yan LL, Yu DY. Utilization of biochar for the removal of nitrogen and phosphorus. J. Cleaner Prod. 2020;257.

28. Dai YH, Zheng H, Jiang ZX, Xing BS. Combined effects of biochar properties and soil conditions on plant growth: A meta-analysis. Sci. Total Environ. 2020;713. https://doi.org/10.1016/j.scitotenv.2020.136635 PMID: 32019022

29. Glaser B, Lehr VI. Biochar effects on phosphorus availability in agricultural soils: A meta-analysis. Sci. Rep. 2019; 9. https://doi.org/10.1038/s41598-019-45693-z PMID: 31249335

30. Melo LCA, Lehmann J, Carneiro JSdS, Camps-Arbestain M. Biochar-based fertilizer effects on crop productivity: A meta-analysis. Plant Soil. 2022; 472(1):45–58.

31. Woolf D, Amonette JE, Street-Perrott FA, Lehmann J, Joseph S. Sustainable biochar to mitigate global climate change. Nat. Comm. 2010; 1(1):56. https://doi.org/10.1038/ncomms1053 PMID: 20975722

32. Lehmann J. A handful of carbon. Nature. 2007; 447(7141):143–4. https://doi.org/10.1038/447143a PMID: 17495905

33. Dunkel C. GHG Emissions and Energy Usage Assessment of Phosphorus Recovery from Municipal Wastewater Systems Using Biochar-Catalytic Oxidation-Reactive Filtration. Moscow, ID: University of Idaho; 2016.

34. Li F, Lianga X, Niyungekoa C, Suna T, Liua F, Arai Y. Effects of biochar amendments on soil phosphorus transformation in agricultural soils. In: Sparks DL, editor. Advances in Agronomy. 158. Amsterdam: Elsevier; 2019.

35. Bakshi S, Fidel R, Banik C, Aller D, Brown RC. 7—Retention of oxyanions on biochar surface. In: Mohan D, Pittman CU, Mlsna TE, editors. Sustainable Biochar for Water and Wastewater Treatment: Elsevier; 2022. p. 233–76.

36. Arai Y, Sparks DL. ATR–FTIR spectroscopic investigation on phosphate adsorption mechanisms at the ferrihydrite–water interface. J Coll. Interface Sci. 2001; 241(2):317–26.

37. Gypser S, Hirsch F, Schleicher AM, Freese D. Impact of crystalline and amorphous iron- and aluminum hydroxides on mechanisms of phosphate adsorption and desorption. Journal Env. Sci. 2018; 70:175–89. https://doi.org/10.1016/j.jes.2017.12.001 PMID: 30037404

38. Parfitt RL, Atkinson RJ, Smart RSC. The mechanism of phosphate fixation by iron oxides. Soil Sci. Soc. Am. J. 1975; 39(5):837–41.

39. Yang Y, Duan P, Schmidt-Rohr K, Pignatello JJ. Physicochemical changes in biomass chars by thermal oxidation or ambient weathering and their impacts on sorption of a hydrophobic and a cationic

compound. Environ. Sci. Technol. 2021; 55(19):13072–81. https://doi.org/10.1021/acs.est.1c04748 PMID: 34555895

40. Wang Z, Bakshi S, Li C, Parikh SJ, Hsieh H-S, Pignatello JJ. Modification of pyrogenic carbons for phosphate sorption through binding of a cationic polymer. J Colloid Interface Sci. 2020; 579:258–68. https://doi.org/10.1016/j.jcis.2020.06.054 PMID: 32592991

41. Deng Y, Li M, Zhang Z, Liu Q, Jiang K, Tian J, et al. Comparative study on characteristics and mechanism of phosphate adsorption on Mg/Al modified biochar. J. Env. Chem. Eng. 2021; 9(2):105079.

42. Kang J-K, Seo E-J, Lee C-G, Park S-J. Fe-loaded biochar obtained from food waste for enhanced phosphate adsorption and its adsorption mechanism study via spectroscopic and experimental approach. J. Env. Chem. Eng. 2021; 9(4):105751.

43. Wang L, Ruiz-Agudo E, Putnis CV, Menneken M, Putnis A. Kinetics of calcium phosphate nucleation and growth on calcite: Implications for predicting the fate of dissolved phosphate species in alkaline soils. Environ. Sci. Technol. 2012; 46(2):834–42. https://doi.org/10.1021/es202924f PMID: 22136106

44. Mood SH, Ayiania M, Jefferson-Milan Y, Garcia-Perez M. Nitrogen doped char from anaerobically digested fiber for phosphate removal in aqueous solutions. Chemosphere. 2020; 240:124889. https://doi.org/10.1016/j.chemosphere.2019.124889 PMID: 31563102

45. Wang L, Putnis CV, Hövelmann J, Putnis A. Interfacial precipitation of phosphate on hematite and goethite. Minerals. 2018; 8(5):207.

46. Ler A, Stanforth R. Evidence for surface precipitation of phosphate on goethite. Environ. Sci. Technol. 2003; 37(12):2694–700. https://doi.org/10.1021/es020773i PMID: 12854707

47. Siciliano A, Limonti C, Curcio GM, Molinari R. Advances in struvite precipitation technologies for nutrients removal and recovery from aqueous waste and wastewater. Sustainability. 2020; 12(18):7538.

48. Hertzberger AJ, Cusick RD, Margenot AJ. A review and meta-analysis of the agricultural potential of struvite as a phosphorus fertilizer. Soil Sci. Soc. Am. J. 2020; 84(3):653–71.

49. Wang JL, Bai ZY. Fe-based catalysts for heterogeneous catalytic ozonation of emerging contaminants in water and wastewater. Chem. Eng. J. 2017; 312:79–98.

50. Liu FL, Zuo JE, Chi T, Wang P, Yang B. Removing phosphorus from aqueous solutions by using iron-modified corn straw biochar. Front. Environ. Sci. Eng. 2015; 9(6):1066–75.

51. Zhou HG, Jiang ZM, Wei SQ. A novel absorbent of nano-Fe loaded biomass char and its enhanced adsorption capacity for phosphate in water. J. of Chem. 2013; 4:1–9.

52. Bakshi S, Laird DA, Smith RG, Brown RC. Capture and release of orthophosphate by Fe-modified biochars: Mechanisms and environmental applications. ACS Sustainable Chem. Eng. 2021; 9(2):658–68.

53. Alhujaily A, Mao YZ, Zhang JL, Ifthikar J, Zhang XY, Ma FY. Facile fabrication of Mg-Fe-biochar adsorbent derived from spent mushroom waste for phosphate removal. J. Taiwan Inst. Chem. Eng. 2020; 117:75–85.

54. Wu L, Zhang S, Wang J, Ding X. Phosphorus retention using iron (II/III) modified biochar in saline-alkaline soils: Adsorption, column and field tests. Environ. Pollut. 2020; 261:114223. https://doi.org/10.1016/j.envpol.2020.114223 PMID: 32109821

55. Min L, Zhongsheng Z, Zhe L, Haitao W. Removal of nitrogen and phosphorus pollutants from water by FeCl3- impregnated biochar. Ecol. Eng. 2020; 149:105792.

56. Peng Y, Sun Y, Fan B, Zhang S, Bolan NS, Chen Q, et al. Fe/Al (hydr)oxides engineered biochar for reducing phosphorus leaching from a fertile calcareous soil. J. Cleaner Prod. 2021; 279:123877.

57. Zhang M, Lin K, Li X, Wu L, Yu J, Cao S, et al. Removal of phosphate from water by paper mill sludge biochar. Environ. Pollut. 2022; 293:118521. https://doi.org/10.1016/j.envpol.2021.118521 PMID: 34793910

58. Yin QQ, Liu MT, Ren HP. Removal of ammonium and phosphate from water by Mg-modified biochar: Influence of Mg pretreatment and pyrolysis temperature. Bioresources. 2019; 14(3):6203–18.

59. Zheng Q, Yang L, Song D, Zhang S, Wu H, Li S, et al. High adsorption capacity of Mg–Al-modified biochar for phosphate and its potential for phosphate interception in soil. Chemosphere. 2020; 259:127469. https://doi.org/10.1016/j.chemosphere.2020.127469 PMID: 32640377

60. Li R, Wang JJ, Zhang Z, Awasthi MK, Du D, Dang P, et al. Recovery of phosphate and dissolved organic matter from aqueous solution using a novel CaO-MgO hybrid carbon composite and its feasibility in phosphorus recycling. Sci. Total Environ. 2018; 642:526–36. https://doi.org/10.1016/j.scitotenv.2018.06.092 PMID: 29908511

61. Dalahmeh SS, Stenstrom Y, Jebrane M, Hylander LD, Daniel G, Heinmaa I. Efficiency of iron- and calcium-impregnated biochar in adsorbing phosphate from wastewater in onsite wastewater treatment systems. Front. Env. Sci. 2020; 8.

62. Fang C, Zhang T, Li P, Jiang RF, Wang YC. Application of magnesium modified corn biochar for phosphorus removal and recovery from swine wastewater. Int. J. Env. Res. Public Health. 2014; 11 (9):9217–37. https://doi.org/10.3390/ijerph110909217 PMID: 25198685

63. Zhang JS, Zhang YS, Zhao WQ, Li ZM, Zang LH. Facile fabrication of calcium-doped carbon for efficient phosphorus adsorption. ACS Omega. 2021; 6(1):327–39. https://doi.org/10.1021/acsomega.0c04642 PMID: 33458484

64. Jung K-W, Ahn K-H. Fabrication of porosity-enhanced MgO/biochar for removal of phosphate from aqueous solution: Application of a novel combined electrochemical modification method. Bioresour. Technol. 2016; 200:1029–32. https://doi.org/10.1016/j.biortech.2015.10.008 PMID: 26476871

65. Huang Q, Luo K, Pi Z, He L, Yao F, Chen S, et al. Zirconium-modified biochar as the efficient adsorbent for low-concentration phosphate: performance and mechanism. Env. Sci. Poll. Res. 2022. https://doi.org/10.1007/s11356-022-20088-2 PMID: 35397030

66. Huang Q, Luo K, Pi Z, He L, Yao F, Chen S, et al. Zirconium-modified biochar as the efficient adsorbent for low-concentration phosphate: performance and mechanism. Environ. Sci. Pollut. Res. Int. 2022. Epub 20220409. https://doi.org/10.1007/s11356-022-20088-2 PMID: 35397030

67. Yi Y, Huang Z, Lu B, Xian J, Tsang EP, Cheng W, et al. Magnetic biochar for environmental remediation: A review. Bioresour. Technol. 2020; 298:122468. https://doi.org/10.1016/j.biortech.2019.122468 PMID: 31839494

68. Li XP, Wang CB, Zhang JG, Liu JP, Liu B, Chen GY. Preparation and application of magnetic biochar in water treatment: A critical review. Sci. Total Environ. 2020; 711. https://doi.org/10.1016/j.scitotenv.2019.134847 PMID: 31812432

69. Zhao QS, Xu T, Song XP, Nie SX, Choi SE, Si CL. Preparation and application in water treatment of magnetic biochar. Front. Bioeng. Biotech. 2021; 9. https://doi.org/10.3389/fbioe.2021.769667 PMID: 34760880

70. Liu Y, Jin J, Li J, Zou Z, Lei R, Sun J, et al. Enhanced phosphorus recovery as vivianite from anaerobically digested sewage sludge with magnetic biochar addition. Sustainability. 2022; 14(14):8690.

71. Kubar AA, Huang Q, Sajjad M, Yang C, Lian FQ, Wang JF, et al. The Recovery of Phosphate and Ammonium from Biogas Slurry as Value-Added Fertilizer by Biochar and Struvite Co-Precipitation. Sustainability. 2021; 13(7).

72. Garcia-Perez M, Apasiku MAA, Mood HS, Mcewen J-S, inventors; 20220081323, assignee. Amorphous carbons for phosphate removal and methods thereof. United States. patent US20220081323A1. 2021.

73. Nageshwari K, Chang SX, Balasubramanian P. Integrated electrocoagulation-flotation of microalgae to produce Mg-laden microalgal biochar for seeding struvite crystallization. Sci. Rep. 2022; 12 (1):11463. https://doi.org/10.1038/s41598-022-15527-6 PMID: 35794246

74. Zhang ZR, Yu HQ, Zhu RX, Zhan X, Yan LG. Phosphate adsorption performance and mechanisms by nanoporous biochar-iron oxides from aqueous solutions. Environ. Sci. Pollution Res. 2020; 27 (22):28132–45. https://doi.org/10.1007/s11356-020-09166-5 PMID: 32410193

75. Amonette JE, Blanco-Canqui H, Hassebrook C, Laird DA, Lal R, Lehmann J, et al. Integrated biochar research: A roadmap. J. Soil Water Cons. 2021; 76(1):24a–9a.

76. Kopecký M, Kolář L, Konvalina P, Strunecký O, Teodorescu F, Mráz P, et al. Modified biochar-A tool for wastewater treatment. Energies. 2020; 13(20):5270.

77. Wang C, Luo D, Zhang X, Huang R, Cao Y, Liu G, et al. Biochar-based slow-release of fertilizers for sustainable agriculture: A mini review. Env. Sci. Ecotech. 2022; 10:100167.

78. An X, Wu Z, Liu X, Shi W, Tian F, Yu B. A new class of biochar-based slow-release phosphorus fertilizers with high water retention based on integrated co-pyrolysis and co-polymerization. Chemosphere. 2021; 285:131481. https://doi.org/10.1016/j.chemosphere.2021.131481 PMID: 34265721

79. Gelardi DL, Parikh SJ. Soils and beyond: Optimizing sustainability opportunities for biochar. Sustainability. 2021; 13(18):10079.

80. Zhang M, Song G, Gelardi DL, Huang L, Khan E, Mašek O, et al. Evaluating biochar and its modifications for the removal of ammonium, nitrate, and phosphate in water. Water Res. 2020; 186:116303. https://doi.org/10.1016/j.watres.2020.116303 PMID: 32841930

81. Taslakyan L, Baker MC, Shrestha DS, Strawn DG, Möller G. CO2e footprint and eco-impact of ultralow phosphorus removal by hydrous ferric oxide reactive filtration: A municipal wastewater LCA case study. Water Environ. Res. 2022; 94(8):e10777. https://doi.org/10.1002/wer.10777 PMID: 36004674

82. Bansal RC, Goyal M. Activated carbon adsorption: CRC press; 2005.

83. Enders A, Lehmann J. Comparison of wet-digestion and dry-ashing methods for total elemental analysis of biochar. Commun. Soil Sci. Plant Anal. 2012; 43(7):1042–52.

84. Graetz DA, Nair VD. Phosphorus Sorption Determination. In: J.L. K, Pierzynski GM, editors. Methods of Phosphorus Analysis for soils, sediments, residuals, and waters. Second: Southern Cooperative Series Bulletin; 2009.

85. Hingston FJ, Quirk JP, Posner AM. Anion adsorption by goethite and gibbsite.1. Role of proton in determining adsorption envelopes. J. Soil Sci. 1972; 23(2):177.

86. Murphy J, Riley JP. A modified single solution method for the determination of phosphate in natural waters. Anal. Chim Acta. 1962; 27:31–6.

87. Pote DH, Daniel TC. Dissolved Phosphorus in Water Samples. In: aGMP Kovar J.L., editor. Methods of Phosphorus Analysis for soils, sediments, residuals, and waters. 2nd: Southern Cooperative Series Bulletin.

88. Strawn DG, Bohn HL, O'Connor GA. Soil Chemistry. Hoboken, NJ: John Wiley & Sons; 2020.

89. Strawn DG, Sparks DL. Effects of soil organic matter on the kinetics and mechanisms of Pb(II) sorption and desorption in soil. Soil Sci. Soc. Am. J. 2000; 64(1):144–56.

90. Ravel B, Newville M. Athena, Artemis, Hephaestus: Data analysis for X-ray absorption spectroscopy using IFEFFIT. J. Synchrotron Rad. 2005; 12:537–41. https://doi.org/10.1107/S0909049505012719 PMID: 15968136

91. Gustafsson JP, Braun S, Tuyishime JRM, Adediran GA, Warrinnier R, Hesterberg D. A probabilistic approach to phosphorus speciation of soils using P K-edge XANES spectroscopy with linear combination fitting. Soil Syst. 2020; 4(2):26.

92. Ingall ED, Brandes JA, Diaz JM, de Jonge MD, Paterson D, McNulty I, et al. Phosphorus K-edge XANES spectroscopy of mineral standards. J. Synchrotron Rad. 2011; 18(2):189–97. https://doi.org/10.1107/S0909049510045322 PMID: 21335905

93. Singh B, Mm D, Shen Q, Camps Arbestain M. Chapter 3. Biochar pH, electrical conductivity and liming potential. n Singh B, Camps-Arbestain M, Johannes Lehmann, editors. Biochar: A guide to analytical methods. Boca Raton, FL, USA: CRC Press; 2017. p. 23–38.

94. Little SN, Shainsky LJ. Distriubtion of Biomass and Nutrients in Lodgepole Pine/Bitterbrush Ecosystems in Central Oregon. In: Costa R, Daniels SJ, editors. Red-Cockaded Woodpecker: Road to Recovery. Blaine, WA: Hancock House Publishers; 1992. p. 633–45.

95. Singh B, Camps-Arbestain M, Lehmann J. Biochar: A Guide to Analytical Methods. Boca Raton, FL, USA: CRC Press; 2017.

96. Gunary D. A new adsorption isotherm for phosphate in soil. J. Soil Sci. 1970; 21(1):72–7.

97. Mead J. A comparison of the Langmuir, Freundlich and Temkin equations to describe phosphate adsorption properties of soils. Soil Research. 1981; 19(3):333–42.

98. Veith JA, Sposito G. On the use of the Langmuir equation in the interpretation of "adsorption" phenomena. Soil Sci. Soc. Am. J. 1977; 41(4):697–702.

99. Werner F, Prietzel J. Standard protocol and quality assessment of soil phosphorus speciation by P K-edge XANES spectroscopy. Environ. Sci. Technol. 2015; 49(17):10521–8. https://doi.org/10.1021/acs.est.5b03096 PMID: 26270570

100. Prietzel J, Harrington G, Hausler W, Heister K, Werner F, Klysubun W. Reference spectra of important adsorbed organic and inorganic phosphate binding forms for soil P speciation using synchrotron-based K-edge XANES spectroscopy. J. Synchrotron Rad. 2016; 23(2):532–44. https://doi.org/10.1107/S1600577515023085 PMID: 26917141

101. Hesterberg D, McNulty I, Thieme J. Speciation of soil phosphorus assessed by XANES spectroscopy at different spatial scales. J. Env. Qual. 2017; 46(6):1190–7. https://doi.org/10.2134/jeq2016.11.0431 PMID: 29293859

102. Beauchemin S, Hesterberg D, Chou J, Beauchemin M, Simard RR, Sayers DE. Speciation of phosphorus in phosphorus-enriched agricultural soils using X-ray absorption near-edge structure spectroscopy and chemical fractionation. J. Env.Qual. 2003; 32(5):1809–19. https://doi.org/10.2134/jeq2003.1809 PMID: 14535324

103. Hansen JC, Strawn DG. Kinetics of phosphorus release from manure-amended alkaline soil. Soil Sci. 2003; 168(12):869–79.

104. Chow LC. Solubility of calcium phosphates. Monogr. Oral Sci. 2001; 18:94–111. https://doi.org/10.1159/000061650 PMID: 11758450

105. Simonsson M, Östlund A, Renfjäll L, Sigtryggsson C, Börjesson G, Kätterer T. Pools and solubility of soil phosphorus as affected by liming in long-term agricultural field experiments. Geoderma. 2018; 315:208–19.

106. Murrmann RP, Peech M. Effect of pH on labile and soluble phosphate in soils. Soil Sci. Soc. Am. J. 1969; 33(2):205–10.

107. Sundman A, Karlsson T, Sjöberg S, Persson P. Impact of iron–organic matter complexes on aqueous phosphate concentrations. Chem. Geol. 2016; 426:109–17.

108. Larsen S. Soil Phosphorus. In: Norman AG, editor. Advances in Agronomy. 19: Academic Press; 1967. p. 151–210.

109. George TS, Fransson A-M, Hammond JP, White PJ. Phosphorus Nutrition: Rhizosphere Processes, Plant Response and Adaptations. In: Bünemann E, Oberson A, Frossard E, editors. Phosphorus in Action: Biological Processes in Soil Phosphorus Cycling. Berlin, Heidelberg: Springer Berlin Heidelberg; 2011. p. 245–71.

110. Hilger DM, Hamilton JG, Peak D. The influences of magnesium upon calcium phosphate mineral formation and structure as monitored by X-ray and vibrational spectroscopy. Soil Syst. 2020; 4(1):8.

111. Barrow NJ. A mechanistic model for describing the sorption and desorption of phosphate by soil. J. Soil Sci. 1983; 34(4):733–50.

112. Kizito S, Luo H, Wu S, Ajmal Z, Lv T, Dong R. Phosphate recovery from liquid fraction of anaerobic digestate using four slow pyrolyzed biochars: Dynamics of adsorption, desorption and regeneration. J Environ. Manage. 2017; 201:260–7. https://doi.org/10.1016/j.jenvman.2017.06.057 PMID: 28672198

113. Weyers E, Strawn DG, Peak D, Baker LL. Inhibition of phosphorus sorption on calcite by dairy manure-sourced DOC. Chemosphere. 2017; 184:99–105. https://doi.org/10.1016/j.chemosphere.2017.05.141 PMID: 28582769

114. Zhang Z, Xu Z, Song X, Zhang B, Li G, Huda N, et al. Membrane processes for resource recovery from anaerobically digested livestock manure effluent: Opportunities and challenges. Curr. Pollut. Rep. 2020; 6(2):123–36.

115. Sörengård M, Östblom E, Köhler S, Ahrens L. Adsorption behavior of per- and polyfluoralkyl substances (PFASs) to 44 inorganic and organic sorbents and use of dyes as proxies for PFAS sorption. J. Environ. Chem. Eng. 2020; 8(3):103744.